

Palmitoylation-Induced Conformational Changes of Specific Side Chains in the Gramicidin Transmembrane Channel[†]

Roger E. Koeppe II,^{*,‡} J. Antoinette Killian,[§] T. C. Bas Vogt,[§] Ben de Kruijff,[§] M. Jeffrey Taylor,[‡]
Gwendolyn L. Mattice,[‡] and Denise V. Greathouse[‡]

Department of Chemistry and Biochemistry, University of Arkansas, Fayetteville, Arkansas 72701, and Department of Biochemistry of Membranes, Center for Biomembranes and Lipid Enzymology, University of Utrecht, Padualaan 8, 3584 CH Utrecht, The Netherlands

*Received January 19, 1995; Revised Manuscript Received May 11, 1995**

ABSTRACT: To gain insight into the structural consequences of acylation for membrane proteins, we have covalently attached palmitic acid to the ethanolamine end of gramicidin A (gA), which functions as a well-characterized cation-selective membrane channel. Next, we investigated by NMR methods the effect of acylation on the side chains of Trp⁹, Leu¹⁰, and Trp¹¹, which are expected to be close to the acyl chain, and of Val⁷, which is expected to be far from the acyl chain. Two-dimensional NMR spectroscopy in a sodium dodecyl sulfate (SDS) environment suggests that one of the β -hydrogens of Leu¹⁰ of gA is severely shielded by a nearby aromatic ring. This shielding disappears upon acylation. Deuterium NMR spectra for labeled samples in hydrated dimyristoylphosphatidylcholine (DMPC) bilayers show that, for the major gA conformation, the (deuterated) side chains of Trp⁹ and Leu¹⁰ are markedly influenced by acylation, whereas the side chains of Val⁷ and Trp¹¹ are essentially unaffected. The NMR results in both environments suggest that the indole ring of Trp⁹ is situated near the side chain of Leu¹⁰ and moves away upon acylation. We propose that acylation provides a subtle mechanism to modulate protein and lipid interactions and to regulate the stability and function of proteins within membranes.

A large number of proteins in cells are modified by a covalently attached fatty acid [for a review, see Schmidt (1989)]. The most common forms of acylation are myristoylation, which occurs via an amide bond on an N-terminal glycine and is often encountered in water-soluble proteins, and palmitoylation, which is more commonly found in membrane proteins and can occur by means of an ester bond to threonine or a thioester bond to cysteine. Little is known about the structural and functional consequences of acylation. It can be expected, however, that the acyl chain will influence protein folding and/or localization, which in turn would affect function. Particularly intriguing is the situation where palmitic acid is attached to a part of a protein that is already embedded in a membrane. Examples include the hydrophobic surfactant protein Sp-C (Beers & Fisher, 1992) and rhodopsin (O'Brien et al., 1987; Ovchinnikov et al., 1988), both of which are palmitoylated at two cysteines, and the membrane-bound form of acetylcholinesterase (Randall, 1994).

To gain insight into the possible consequences of palmitoylation for protein structure and function, we have used gramicidin A (gA)¹ as a model. Gramicidin is hydrophobic and forms membrane channels by hydrogen bonding at the formyl NH-terminals of two gA monomers, each present in the $\beta^6.3$ -helical conformation and spanning half of a bilayer

membrane (Urry, 1971; Cifu et al., 1992). The conformational and channel-forming properties of gA are well studied and understood [for recent reviews see Andersen and Koeppe (1992) and Killian (1992)]. Gramicidin A is also interesting as a model acylprotein, because it occurs naturally in both free and acylated forms, the latter consisting of a fatty acid esterified to the hydroxyl group of the C-terminal ethanolamine (Koeppe et al., 1985). This ethanolamine acylation site can be used for the chemical attachment of acyl chains (Vogt et al., 1991), and its interfacial localization (Arsen'ev et al., 1986; Koeppe et al., 1992) mimics the location of the acylation site in palmitoylated membrane proteins.

Functionally, the acylation of gA does not alter the single-channel conductance for Na⁺ or Cs⁺, but it does increase the mean channel lifetime 5-fold (Koeppe et al., 1985; Vogt et al., 1992). Previous studies have demonstrated that acylation does not notably affect the structure of the gA backbone (Vogt et al., 1991, 1992; Koeppe et al., 1992; Williams et al., 1992). Nothing is known about the possible influence of acylation on the orientation and dynamics of side chains. Yet this is an important consideration, because modulations of side chains could relate to the increased mean gA channel lifetime and could provide a general mechanism for regulating both the function of acylproteins and their interactions with lipids and other proteins.

Deuterium NMR studies of the acyl chain of palmitoyl-gA (Vogt et al., 1994) have shown that the carboxy-terminal part of the acyl chain makes a bend with respect to the helix axis, while the rest of the chain extends down parallel to the helix axis and the surrounding phospholipids. When viewed from the end of the gA channel (Figure 1), the acylation site on the ethanolamine hydroxyl lies above residue Leu¹⁰.

[†] This work was supported in part by NIH Grant GM34968 from the U.S. Public Health Service and NSF Grant EHR-9108762.

[‡] University of Arkansas.

[§] University of Utrecht.

^{*} Abstract published in *Advance ACS Abstracts*, July 1, 1995.

¹ Abbreviations: gA, gramicidin A; SDS, sodium dodecyl sulfate; DMPC, dimyristoylphosphatidylcholine; COSY, correlated spectroscopy; NOESY, nuclear Overhauser enhancement spectroscopy.

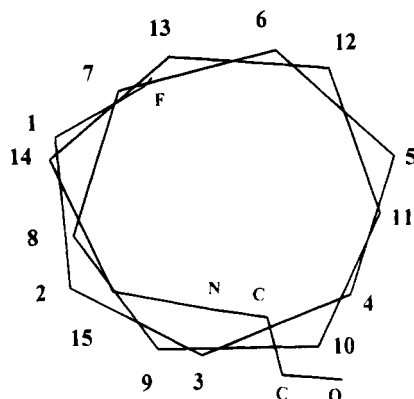


FIGURE 1: Helical wheel representation of the right-handed gramicidin $\beta^{6.3}$ helix based on the backbone of an energy-minimized model (Killian et al., 1992). The diagram shows projections of the positions of the C α carbons of one monomer (numbered), the formyl group (F), and the ethanolamine (N—C—C—O) site to which the acyl chain in palmitoylgramicidin is attached.

A helical wheel diagram such as that in Figure 1 predicts that the acyl chain should at its bending point run close to the side chain of Leu¹⁰ and perhaps also to Trp⁹ or Trp¹¹. The acyl chain should be far away from Val⁷.

By using ²H-NMR analysis, as described previously (Killian et al., 1992; Koeppel et al., 1994a), of oriented samples of side-chain deuterated gA and palmitoyl-gA in DMPC, and by using two-dimensional ¹H-NMR spectra for micellar systems, we have investigated the effect of acylation on both the backbone structure and the orientations and dynamics of the side chains of Val⁷, Trp⁹, Leu¹⁰, and Trp¹¹. The results demonstrate that the covalently coupled acyl chain induces site-specific changes in the side-chain orientations for Trp⁹ and Leu¹⁰ but not for the backbone or for Val⁷ or Trp¹¹. We will discuss the implications of these results for the gramicidin channel and for membrane-associated acylproteins in general.

MATERIALS AND METHODS

The deuterated materials, L-Val-*d*₈, L-Leu-*d*₁₀, L-Trp-*ring-d*₅ and SDS-*d*₂₅, were from Cambridge Isotope Laboratories (Andover, MA). The SDS-*d*₂₅ was recrystallized from 95% ethanol.

[Trp⁹-*d*₅]gA, [Trp¹¹-*d*₅]gA, and [Val⁷-*d*₈]gA were prepared as previously described (Koeppel et al., 1994a). For the labeling of Leu¹⁰, the enantiomer, gA[−] (Koeppel et al., 1992), was synthesized because of the availability of the L-Leu-*d*₁₀ isomer. The single-channel properties of gA[−] are identical to those of gA (Koeppel et al., 1992), and the use of gA[−] rather than gA does not influence our conclusions regarding the side chain of Leu¹⁰. [Ala¹,D-Ala²]gA was synthesized as in Mattice et al. (1995).

Fifty milligrams of each labeled gA sample was acylated with palmitic acid, and purified, using the methods of Vogt et al. (1991).

Oriented, hydrated samples of 30 μ mol of DMPC and 3 μ mol of labeled (acyl)gA were prepared between glass plates, as previously described (Killian et al., 1992). ³¹P-NMR spectra indicated that the lipids in the bilayers became well aligned following 48–72 h of incubation at 40 °C. ²H-NMR spectra were recorded at 40° or 50 °C as previously described (Killian et al., 1992), using the quadrupolar echo sequence (Davis et al., 1976) on a Bruker MSL 300 or Bruker AMX

300 spectrometer with a 7.5 mm diameter solenoid coil. A total of 0.5–1.5 million scans were accumulated while employing a 4 μ s 90° pulse, a 50–200 ms interpulse time, and a 60 μ s echo delay time. The signal-to-noise ratio was increased by applying a line broadening of 200 Hz (Leu, Val) or 1 kHz (Trp) prior to Fourier transformation.

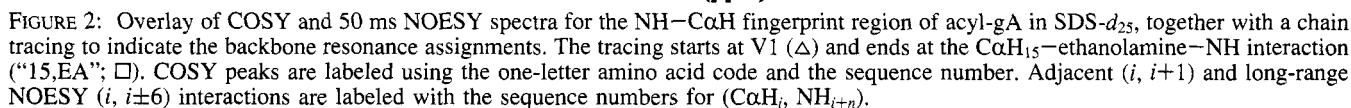
Samples of natural (unlabeled) gA and acyl-gA (isolated from gramicidin K) (Koeppel et al., 1985, 1992) in SDS-*d*₂₅ (50:1 SDS:gramicidin) were prepared for ¹H-NMR spectroscopy by methods previously described for [Val⁵,D-Ala⁸]gA (Koeppel et al., 1994b). Double-quantum-filtered COSY spectra (Rance et al., 1983) were recorded at 55 °C using a 500 MHz Varian VXR 500S spectrometer over a sweep width of 6 kHz. A total of 512 FID of 4K complex points were acquired with 32 scans per *t*₁ value. The NOESY spectra of acyl-gA and [Ala¹,D-Ala²]gA were recorded with mixing times of 50 or 100 ms, using 512 *t*₁ points and 4096 complex *t*₂ points with 64 scans per *t*₁ value. The spectra were zero-filled to a 4K × 4K matrix and processed on a Sun 4/110 computer using VNMR software (Varian). Spectral solvent suppression was accomplished by presaturation.

Figure 10 was prepared using the program InsightII (Biosym Technologies, San Diego, CA) on an Iris-4D computer (Silicon Graphics Corp., Mountain View, CA). The backbone coordinates were from Killian et al. (1992).

RESULTS

gA and Acyl-gA in SDS. Previous two-dimensional ¹H-NMR studies on gA in SDS micelles have demonstrated that the peptide is present as a right-handed $\beta^{6.3}$ helix (Arsen'ev et al., 1985; Tucker et al., 1993). We find that acyl-gA also adopts the $\beta^{6.3}$ -helical conformation. Figure 2 shows an overlay of NOESY and COSY spectra for the NH—C α H “fingerprint” region for the backbone of acyl-gA, including the chain tracing and the sequential assignments of the backbone resonances from Val¹ through the ethanolamine of acyl-gA, obtained by standard methods (Wüthrich, 1986). Also labeled in Figure 2 are the long-range NOESY cross peaks that are indicative of a right-handed $\beta^{6.3}$ helix, NH_{*i*}—C α H_{*i*+6} for even *i* and NH_{*i*}—C α H_{*i*−6} for odd *i* (Arsen'ev et al., 1985; Koeppel et al., 1994b). This NMR evidence for the retention of backbone structure is in agreement with previous data that include the similar circular dichroism spectra of gA and acyl-gA (Vogt et al., 1991) and the hybrid channel formation between acyl-gA and right-handed $\beta^{6.3}$ -helical reference compounds (Williams et al., 1992).

For the side chains of gA, environmental changes can be detected around Leu¹⁰. Figure 3 extends the assignments of the Leu¹⁰, Leu¹², and Leu¹⁴ COSY peaks out to the C β —¹H side-chain resonances for these leucines in acyl-gA. These resonances can then be compared with the corresponding Leu resonances of gA (Arsen'ev et al., 1985, 1986; Tucker et al., 1993). Figure 4 illustrates such a comparison and reveals that the C β —¹H chemical shifts for Leu¹² and Leu¹⁴ of acyl-gA show only small changes from gA, while those of Leu¹⁰ are strongly influenced by acylation (note the 10 β and 10 β' peaks in Figure 4). One Leu¹⁰ C β —¹H resonance is far upfield in gA, at −0.35 ppm (Table 1). Such a negative chemical shift implies that the side chain of Leu¹⁰ in gA is shielded by a nearby aromatic ring. In that case the close vicinity of that aromatic ring may be expected to lead to NOE interactions with Leu¹⁰.



leucine residue	¹ H chemical shift (ppm) ^a	
	gA	acyl-gA
Leu ⁴ Cβ-H	1.58	1.75
	1.87	1.96
Leu ¹⁰ Cβ-H	-0.35	0.51
	0.48	0.74
Leu ¹² Cβ-H	-0.12	-0.05
	0.82	0.87
Leu ¹⁴ Cβ-H	0.24	0.09
	1.22	1.15

^a The chemical shifts are relative to 3-(trimethylsilyl)propionate 2,2,3,3-*d*₄. The resonance assignments for gA are from Arsen'ev et al. (1985).

Upon acylation, the Leu¹⁰ C β -¹H resonance moves to positive chemical shift (as noted above, Figures 3 and 4). In this region of the spectrum it was not possible to detect any aromatic ring NOE interactions with Leu¹⁰. From Table 1 it is clear that Leu¹⁰ goes from being the most highly ring-shielded leucine in gA to being less under the influence of ring current than either Leu¹² or Leu¹⁴ in acyl-gA. We attribute these effects to a relative movement of the Trp⁹ indole ring and the Leu¹⁰ side chain away from each other when the ethanolamine of gA is acylated with a long-chain fatty acid.

Figure 6 shows the difference in the solid-state ^2H -NMR spectra for oriented, hydrated samples of $[\text{Leu}^{10}\text{-d}_{10}]\text{gA}^-$ and palmitoyl- $[\text{Leu}^{10}\text{-d}_{10}]\text{gA}^-$ in DMPC. In these spectra, the samples are oriented at $\beta = 90^\circ$, with the helix axis of gramicidin perpendicular to the magnetic field; due to rapid axial reorientation of the gramicidin channels the quadrupolar splittings at $\beta = 90^\circ$ are 2-fold reduced from those that are observed when $\beta = 0^\circ$ (Killian et al., 1992). A first important observation from these spectra is that in both gA^- and acyl- gA^- the splitting of the backbone deuterium (the outer splitting in Figure 6) is the same. These splittings of

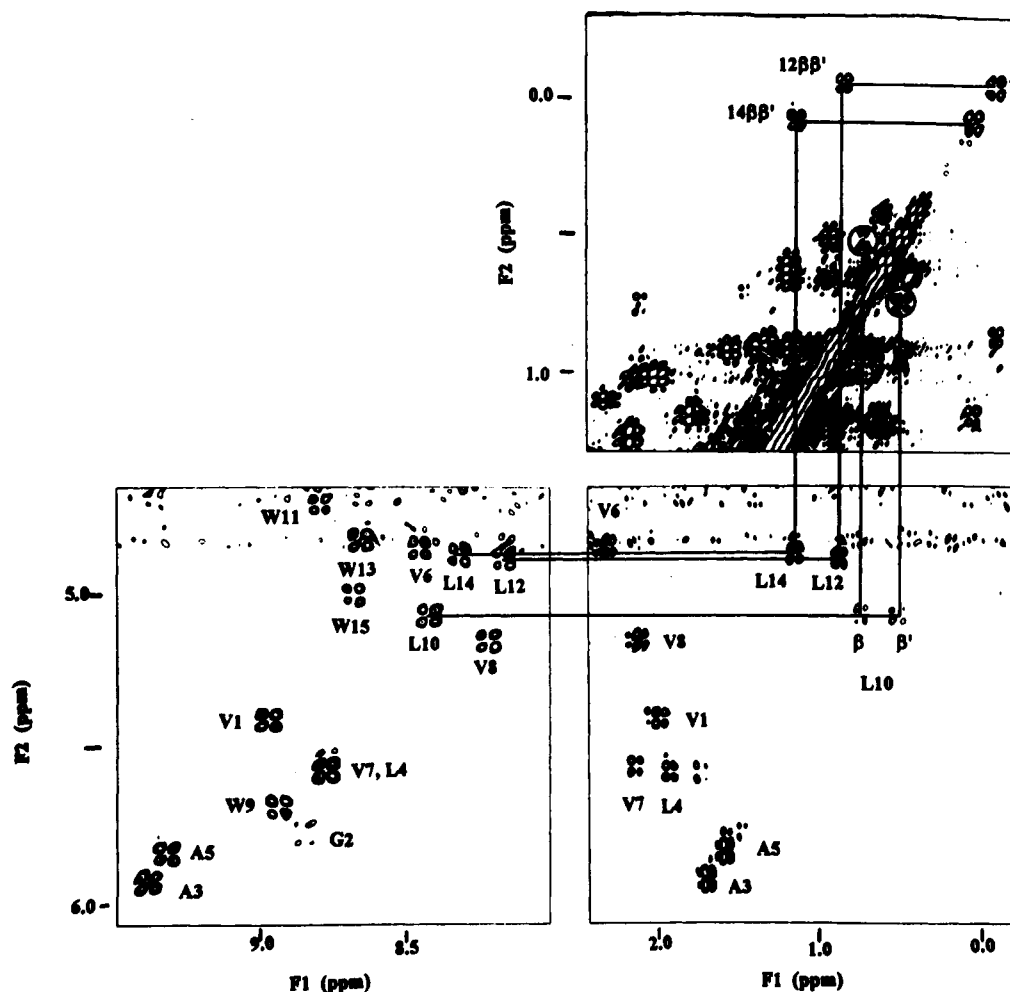


FIGURE 3: Assembled sections of the COSY spectrum of acyl-gA to show the high-field resonance assignments for leucines 10, 12, and 14. For each of these leucines, the backbone COSY peak (lower left), assigned in Figure 2, is connected to an α,β peak and then to a β,β' peak in the high-field region (upper right). The resulting assignments are in agreement with those for acyl-gA in Figure 4.

Table 2: Magnitudes of ^2H Quadrupolar Splittings for Side Chains 7, 9, 10, and 11 of Channel-Form Gramicidin and Acylgramicidin in DMPC Bilayers

residue	^2H quadrupolar splitting (kHz) ^a	
	gA	acyl-gA
Val ⁷ C α	207	204
Val ⁷ C β	78	70
Val ⁷ CD ₃ 's (both)	4	5
Trp ⁹ ring	43	56
	88	79
	104	85
	153	174
Leu ¹⁰ C α	204	204
Leu ¹⁰ C β , C γ	46, 102	48, 60, 84
Leu ¹⁰ CD ₃	14, 30	18, 22
Trp ¹¹ ring	47	53
	84	85
	96	94
	189	191

^a Values are shown for the $\beta = 0^\circ$ molecular orientation; temperature is 50 °C for Val and Leu and 40 °C for Trp. At $\beta = 90^\circ$, the splittings were 2-fold reduced, and there was good agreement between splittings measured in the two orientations. The largest splittings (those above 200 kHz) were measured at $\beta = 90^\circ$ and multiplied by 2 to give the values shown. For Trp⁹ and Trp¹¹ in (nonacylated) gA, see also Hu et al. (1993) and Koeppel et al. (1994a).

204 kHz at $\beta = 0^\circ$ (see also Table 2) were assigned to the C α deuteron of the backbone on the basis of analogy with

other backbone C α deuterons (Hing et al., 1990; Prosser et al., 1991; Killian et al., 1992).

In contrast to the backbone deuteron, all of the side-chain deuterons of Leu¹⁰ are markedly influenced by acylation. The two pairs of more prominent peaks in the spectra of Figure 6 can be assigned, on the basis of their high intensities and relatively low quadrupolar splittings [e.g., see Killian et al. (1992)], to the two CD₃ groups of Leu¹⁰-d₁₀. These methyl resonances move closer to each other in acyl-gA⁻ (Figure 6A), one appearing at a larger quadrupolar splitting and one at a smaller splitting than in gA⁻ prior to acylation (Figure 6B).

Also the C β and C γ Leu¹⁰ side-chain deuterons, which account for the remaining three individual resonances, are affected by acylation. In gA (Figure 6B) these resonances are not resolved but are represented by two broad low-intensity peaks in the region between ± 10 and 25 kHz. The remaining resonance could be underlying or merged with one of the other peaks. In acyl-gA, the C β -D and C γ -D resonances appear at new positions, and are more clearly resolved, so that all three individual peaks are seen.

The quadrupolar splittings of all deuterons before and after acylation are summarized in Table 2. The changes in the positions of the side-chain ^2H resonances, for both the methyls and the C-D groups, indicate that the Leu¹⁰ side chain experiences a different average conformation following the covalent palmitoylation.

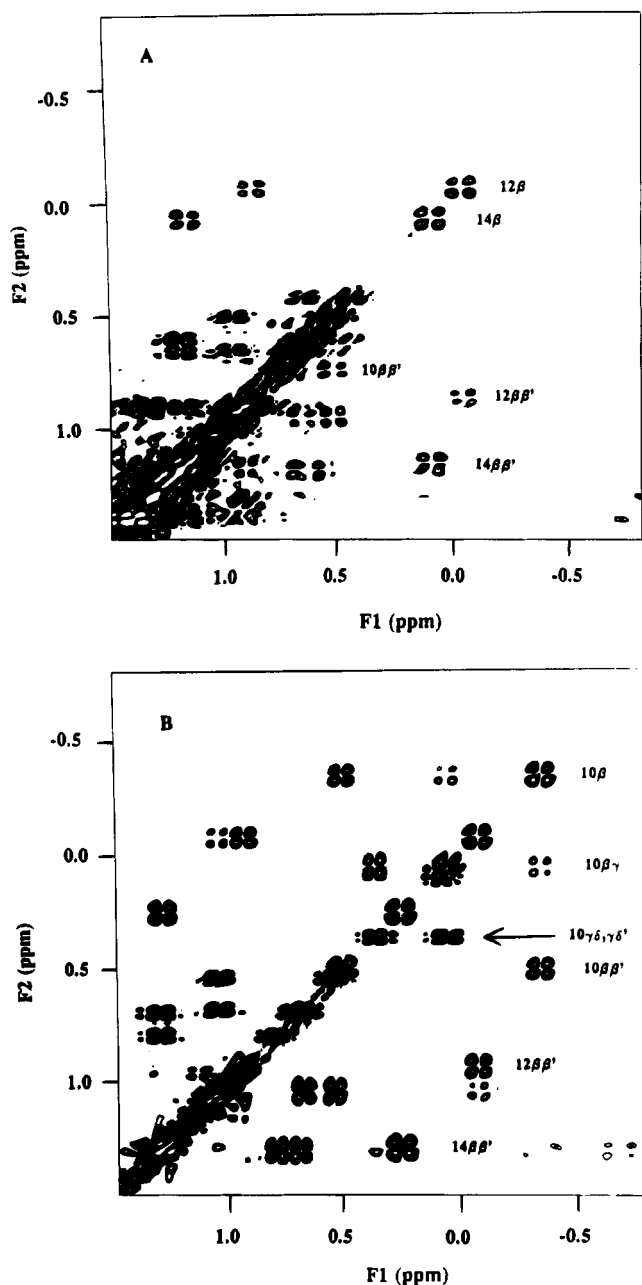


FIGURE 4: High-field aliphatic COSY spectrum of (A) natural acyl-gA (isolated from "gramicidin K") in SDS- d_{25} micelles at 55 °C and (B) nonacylated natural gA under the same conditions. Selected cross peaks are labeled. The Leu¹⁰ β and γ resonances move significantly, whereas the β , β' , and γ resonances of leucines 12 and 14 are little affected by acylation.

A similar effect is observed for the indole ring of Trp⁹, as reported by the deuterons of [Trp⁹- d_5]gA in the spectra shown in Figure 7. At 40 °C, the largest quadrupolar splitting for [Trp⁹- d_5]gA increases from 153 to 174 kHz upon acylation (Table 2). The two middle resonances move closer together (and are coincident at 50 °C), and the smallest quadrupolar splitting increases. This suggests that the indole ring of Trp⁹ is significantly influenced by the presence of the palmitoyl chain.

In contrast, Figure 8 shows that the indole ring of Trp¹¹ is little affected by acylation. Although there are small changes in some of the relative resonance intensities, which are not understood at this time, the positions of the ^2H resonances are very nearly the same in the spectra for Trp¹¹ before and

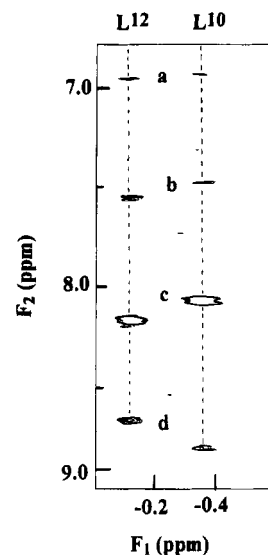


FIGURE 5: Portion of a NOESY spectrum (100 ms mixing time) of [Ala¹,D-Ala²]gA in SDS- d_{25} . The L¹² peaks are due to Leu¹² C β - ^1H interactions with (a) Trp¹³ C ζ 3- ^1H , (b) Trp¹³ C ϵ 3- ^1H , and the backbone N- ^1H 's of (c) Leu¹² and (d) Trp¹³. The L¹⁰ peaks are due to Leu¹⁰ C β - ^1H interactions with (a) Trp⁹ C ζ 3- ^1H , (b) Trp⁹ C ϵ 3- ^1H , and the backbone N- ^1H 's of (c) Leu¹⁰ and (d) Trp¹¹ [assignments from Mattice (1994)]. We have been unable to detect the corresponding interactions for Trp⁹ with Leu¹⁰ in acyl-gA.

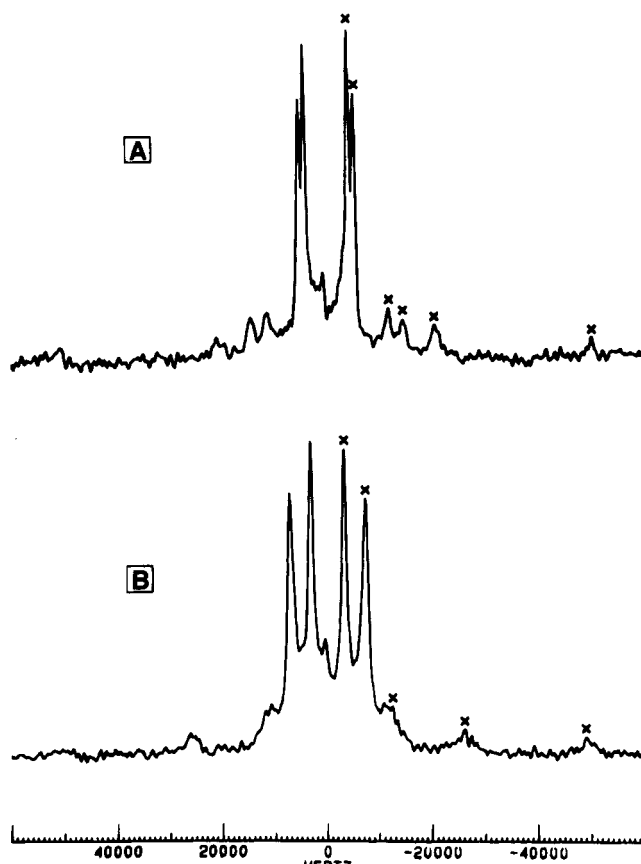


FIGURE 6: ^2H -NMR spectra before and after palmitoylation for [Leu¹⁰- d_{10}]gA⁻ in DMPC bilayers that have been oriented at $\beta = 90^\circ$ at a temperature of 50 °C: (A) acyl-gA; (B) gA.

after acylation. This observation is striking in view of the strong effect of acylation upon the Trp⁹ and Leu¹⁰ side chains.

As a further control, the acylation of [Val⁷- d_8]gA was investigated. Figure 9 shows spectra for oriented samples of [Val⁷- d_8]gA in DMPC, before and after acylation. In each

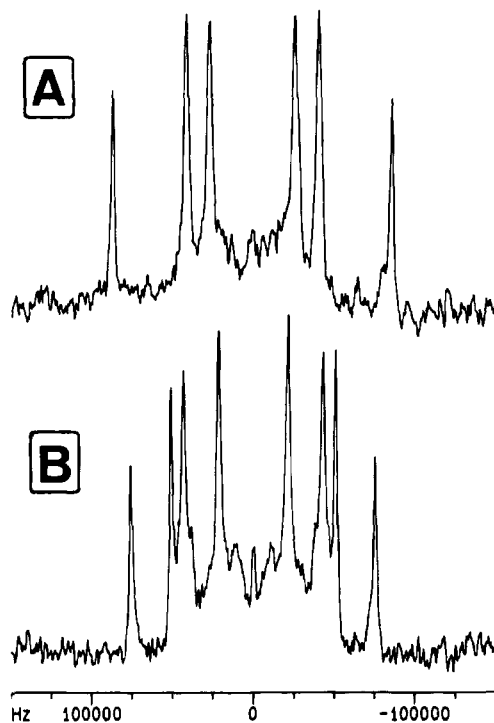


FIGURE 7: ^2H -NMR spectra before and after palmitoylation for $[\text{Trp}^9\text{-}d_5]\text{gA}$ in DMPC bilayers that have been oriented at $\beta = 0^\circ$ at a temperature of 50°C : (A) acyl-gA; (B) gA.

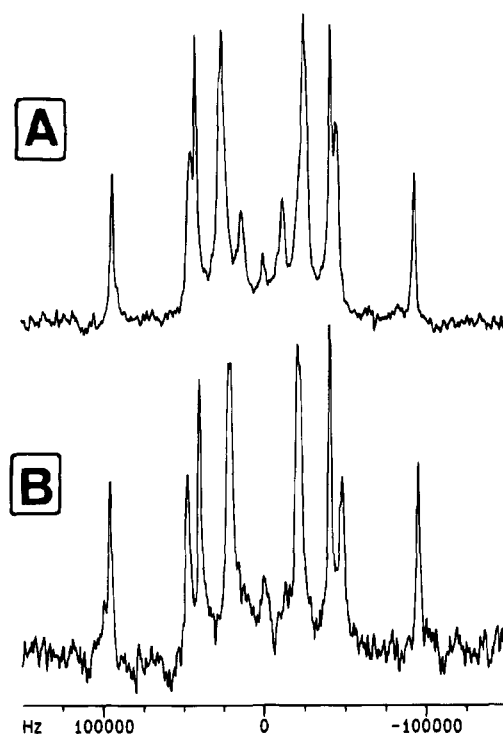


FIGURE 8: ^2H -NMR spectra before and after palmitoylation for $[\text{Trp}^{11}\text{-}d_5]\text{gA}$ in DMPC bilayers that have been oriented at $\beta = 0^\circ$ at a temperature of 50°C : (A) acyl-gA; (B) gA. (The peaks at ± 13 kHz in panel A are due to a small amount of nonoriented sample.)

spectrum, the two valine CD_3 groups are represented by the single pair of tall peaks in the center (Figure 9). The overlap of the methyl resonances was confirmed by temperature-dependent measurements which showed that, for both gA and acyl-gA, the $\text{Val}^7\text{-}d_8$ CD_3 resonances are distinguishable at some temperatures and not at others (data not shown).

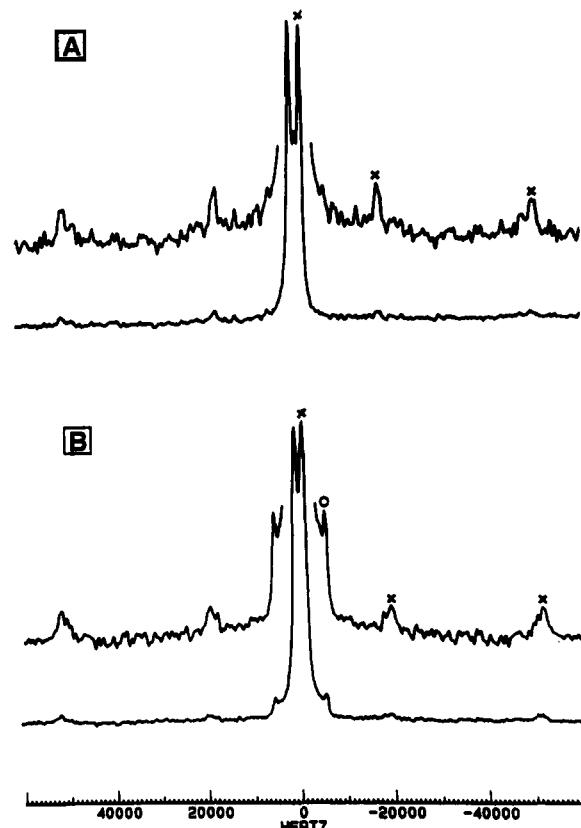


FIGURE 9: ^2H -NMR spectra before and after palmitoylation for $[\text{Val}^7\text{-}d_8]\text{gA}$ in DMPC bilayers that have been oriented at $\beta = 90^\circ$ at a temperature of 50°C : (A) acyl-gA; (B) gA. The upper spectrum in each case results from symmetrization and $5\times$ vertical expansion of the corresponding lower spectrum.

The CD_3 resonances for Val^7 show very little change on acylation.

In the expanded and symmetrized spectra of Figure 9 are seen the resonances due to the $\text{C}\alpha$ and $\text{C}\beta$ deuterons of Val^7 of gA and acyl-gA. Both pairs of splittings show only very small changes on acylation (Figure 9, Table 2). The most obvious difference between the spectra in Figure 9 is the presence of an extra peak *before* acylation (marked o in Figure 9B). We attribute this peak to the presence of a minor conformation for gA or for the Val^7 side chain, which disappears upon acylation.

Taken together, the ^2H -NMR spectra (Figures 6–9) show that there are specific conformational and/or motional changes for the side chains of Trp^9 and Leu^{10} when gramicidin channels are acylated with palmitic acid on the ethanolamine hydroxyl. The effects of acylation are negligible or much less dramatic for Val^7 and Trp^{11} .

DISCUSSION

This study demonstrates specific interactions between amino acid side chains and a covalent lipid chain in a functional transmembrane unit: the cation-selective gramicidin channel. As such, these results serve as a prototype for lipid–protein interactions. We will focus on three topics in this discussion: (1) location of the acyl chain in palmitoylgramicidin, (2) structural consequences of the acyl chain, and (3) possible functional consequences of acylation for membrane proteins.

(1) *Location of the Acyl Chain in Palmitoylgramicidin.* Our data (Figures 6–9) clearly show that the ethanolamine-

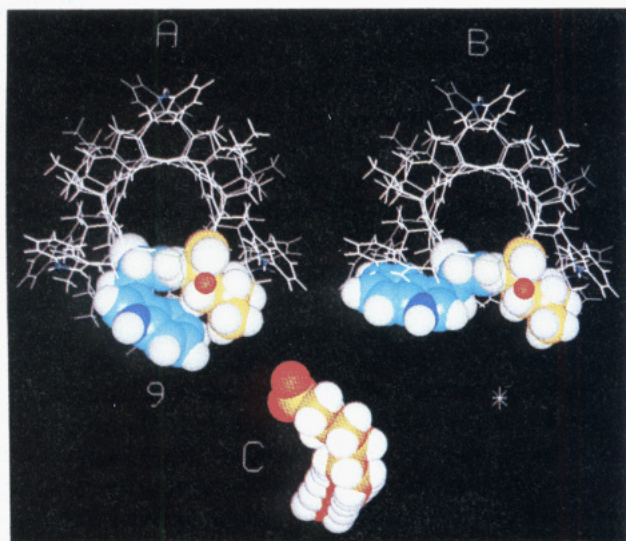


FIGURE 10: Molecular model to show (A) the close proximity of the Trp⁹ (blue) and Leu¹⁰ (yellow) side chains in gA that is deduced from both the ¹H-NMR data (SDS) and the ²H-NMR data (DMPC). In panel A the (χ_1 , χ_2) angles for Trp⁹ are (194°, 92°). Panel B shows an alternative assignment of the gA Trp⁹ orientation (Ketchum et al., 1993), where the (χ_1 , χ_2) angles for Trp⁹ are (260°, 269°). Panel C shows a bent acyl chain in one of the conformations deduced by Vogt et al. (1994); the lower part of the chain would not be all *trans* as shown here but would exhibit motions similar to those of the bulk lipids. In palmitoyl-gA the acyl chain is esterified to the ethanolamine oxygen (the smaller red space-filling atom in panel A or B).

attached palmitoyl group of acyl-gA strongly influences Trp⁹ and Leu¹⁰ but has little effect on Val⁷ or Trp¹¹. These observations allow us to propose a model for the way the palmitoyl chain runs along the outer surface of the channel. The model has the acyl chain proceeding from its attachment site on the ethanolamine OH group, passing over and making van der Waals contact with the side chains of Trp⁹ and Leu¹⁰—and partially separating these side chains—and then continuing down alongside the gramicidin toward the center of the bilayer. The acyl chain is far from Val⁷, and it exerts much less influence on Trp¹¹ than on Trp⁹.

²H-NMR investigations of labels on the palmitoyl chain itself have revealed that carbons 2–6 assume relatively rigid orientations, with a proposed bend in the region of carbons 4–6, and carbons 7–16 behave approximately as bulk lipid (Vogt et al., 1994). The bend between carbons 4–6 allows the acyl chain to follow the contoured outer boundary defined by the Trp⁹ and Leu¹⁰ side chains on the surface of the gramicidin channel. This bend in the acyl chain is depicted diagrammatically in the model of a palmitic acid molecule in Figure 10C.

(2) *Structural Consequences of the Acyl Chain.* The covalent acyl chain has no effect on the backbone structure of gA in its major conformation, the $\beta^{6.3}$ -helical channel conformation. This is shown by the long-range NH–C α H NOESY interactions in the fingerprint region of acyl-gA (Figure 2) and by the unchanged ²H quadrupolar splittings for the C α deuterons of Val⁷ and Leu¹⁰ following acylation (Figures 6, 9).

The acyl chain has no significant effect on the major side-chain conformations of either Val⁷ or Trp¹¹. Also for [Trp¹³-d₅]gA, acylation produces little or no change in the ²H-NMR spectra (Vogt, 1994; R. E. Koeppe II, J. A. Killian, T. C. B. Vogt, and B. de Kruijff, unpublished results). The ²H

quadrupolar splittings are very sensitive to bond orientation. The largest change in Trp¹¹ upon acylation (from 47 to 53 kHz; see Table 2) could be due to a less than 1° change in the orientation of the C–D bond, whereas the change in quadrupolar splitting from 153 to 174 kHz in Trp⁹ (see Table 2) could result from a 4° change in bond orientation, if the spectral assignments do not change [see Hu et al. (1993) and Koeppe et al. (1994a)]. If acylation does change the spectral assignments for Trp⁹, then the changes in ring C–D bond orientations will be correspondingly larger. In any case, it is clear that for Val⁷ and Trp¹¹ the changes are much smaller than for Trp⁹ and Leu¹⁰.

The model in Figure 10A is consistent with the solid-state NMR data. In bilayer-solubilized gA, the Trp⁹ interactions help to assign the Trp⁹ side-chain conformation in *nonacyl*-gA. Solid-state NMR spectra of labeled gramicidins in DMPC (Hu et al., 1993; Koeppe et al., 1994a) are consistent with four sets of (χ_1 , χ_2) values for each Trp side chain. Figure 10A shows the ring of Trp⁹ in an orientation that is consistent with ²H-NMR spectra (Koeppe et al., 1994a) and that places the ring close to the side chain of Leu¹⁰. In the orientation of Figure 10A, the ring current of Trp⁹ will shield Leu¹⁰, consistent with the ¹H-NMR spectra of Figures 4B and 5. It is evident that there is no room for a palmitoyl chain (Figure 10C) in between the side chains of Trp⁹ and Leu¹⁰ in Figure 10A. Figure 10A therefore accurately describes the situation for gA in SDS: the orientations of Trp⁹ and Trp¹¹ match those assigned by Arsen'ev et al. (1986) for gA in SDS and agree with one of the possible orientations for each in DMPC (Hu et al., 1993; Koeppe et al., 1994a).

In bilayer-solubilized gA, one might expect the possibility of differences in the detailed side-chain conformations, due to the very substantial differences in “head group” structure and chain packing between micelles and lipid bilayers. Indeed, Ketchum et al. (1993) have suggested that the side chain of Trp⁹ may adopt a different rotameric state in DMPC than in SDS. This alternative conformation, proposed for Trp⁹ in DMPC, is depicted in Figure 10B. In both panels A and B of Figure 10, the Trp⁹ orientation is consistent with the Raman spectra of Takeuchi et al. (1990), from which it was concluded that χ_2 should be near $\pm 90^\circ$ (in Figure 10A χ_2 is near $+90^\circ$, while in Figure 10B χ_2 is near -90°). Our argument against the orientation in Figure 10B is indirect: the ring of Trp⁹ would already be far away from Leu¹⁰ and there would be plenty of room to accommodate an incoming acyl chain. Therefore, there would seem to be no need for an attached acyl chain to perturb Trp⁹. With the orientation depicted in Figure 10B, it would seem improbable that the acyl chain would simultaneously interact with both Trp⁹ and Leu¹⁰. Yet these are precisely the two side chains whose ²H-NMR spectra in DMPC are perturbed by the acyl chain (Figures 6, 7); remarkably, Trp¹¹—although it is nearby—is not affected by the acyl chain.

Thus, Figure 10A depicts an orientation for Trp⁹ that is consistent with the NMR data for gA in both SDS and DMPC. Together, the data are consistent with tryptophans 9 and 11 being oriented similarly in DMPC to the respective Trp in SDS. While we cannot completely rule out a more complicated behavior in which one or more side chains would orient differently in SDS and DMPC, such a postulate is not necessary to explain our data. The changes that are observed for Trp⁹ and Leu¹⁰ upon acylation favor similar orientations in SDS and DMPC.

(3) *Functional Consequences of Acylation.* The acylation of membrane proteins provides a potential mechanism for regulating the function of such proteins. Interestingly, our studies indicate no effect of acylation on the backbone folding of gA in its major $\beta^{6.3}$ -helical channel conformation. However, a distinct change in average orientation was observed for some of the side chains. These effects could have important implications for interactions with other subunits and other proteins, as well as for lipid-protein interactions.

For instance, it has been demonstrated that the protein side chains play an important role in the association of transmembrane helices (Lemmon et al., 1992). Therefore, a perturbation of specific side chains by a covalently attached acyl chain could alter the helix-helix recognition and packing within a membrane. Alternatively, the covalent acyl chain may pack between side chains along the surface of a membrane protein and serve as a stabilizing "spacer" that interacts favorably with both hydrophobic side chains and membrane lipids. Finally, changes in the orientations of side chains that are involved in hydrogen bonding with lipid carbonyl groups or head groups could change the stabilities and/or functions of larger domains to which the side chains are attached.

For gramicidin, it was shown that the single-channel conductance is unaffected by acylation but that the average lifetime is increased by a factor of 5 (Koeppe et al., 1985; Williams et al., 1992; Vogt et al., 1992). While the precise mechanism remains unknown, it is nevertheless plausible that subtle changes in protein and lipid interactions are responsible for the increased mean lifetime of the acylgramicidin channel dimer. It is tempting to speculate that the minor conformation detected at Val⁷ may represent an alternatively folded backbone or perhaps a part of a "channel unfolding" pathway that is inhibited by acylation.

Summary. This paper reports the first evidence on a molecular level to indicate that modification of a transmembrane protein by a covalently coupled acyl chain can change the orientation and/or dynamics of specific protein side chains. Possible indirect and less dramatic effects on a more distant side chain are also noted. These effects provide a subtle mechanism to regulate protein function. Such regulation could occur either by modulating protein-protein interactions and/or by affecting protein-lipid interactions.

ACKNOWLEDGMENT

We thank Dr. James Hinton for the spectrum in Figure 4B.

REFERENCES

- Andersen, O. S., & Koeppe, R. E., II (1992) *Physiol. Rev.* 72, S89-S158.
- Arsen'ev, A. S., Barsukov, I. L., Bystrov, V. F., Lomize, A. L., & Ovchinnikov, Y. A. (1985) *FEBS Lett.* 186, 168-174.
- Arsen'ev, A. S., Lomize, A. L., Barsukov, I. L., & Bystrov, V. F. (1986) *Biol. Membr.* 3, 1077-1104.
- Beers, M. F., & Fisher, A. B. (1992) *Am. J. Physiol.* 63, 1151-1160.
- Cifu, A., Koeppe, R. E., II, & Andersen, O. S. (1992) *Biophys. J.* 61, 1-15.
- Davis, J. H., Jeffrey, K. R., Bloom, M., Valio, M. I., & Higgs, T. P. (1976) *Chem. Phys. Lett.* 42, 390-394.
- Hing, A. W., Adams, S. P., Silbert, D. F., & Norberg, R. E. (1990) *Biochemistry* 29, 4144-4156.
- Hu, W., Lee, K. C., & Cross, T. A. (1993) *Biochemistry* 32, 7035-7047.
- Ketchum, R. R., Hu, W., & Cross, T. A. (1993) *Science* 261, 1457-1460.
- Killian, J. A. (1992) *Biochim. Biophys. Acta* 1113, 391-425.
- Killian, J. A., Taylor, M. J., & Koeppe, R. E., II (1992) *Biochemistry* 31, 11283-11290.
- Koeppe, R. E., II, Paczkowski, J. A., & Whaley, W. L. (1985) *Biochemistry* 24, 2822-2826.
- Koeppe, R. E., II, Providence, L. L., Greathouse, D. V., Heitz, F., Trudelle, Y., Purdie, N., & Andersen, O. S. (1992) *Proteins* 12, 49-62.
- Koeppe, R. E., II, Killian, J. A., & Greathouse, D. V. (1994a) *Biophys. J.* 66, 14-24.
- Koeppe, R. E., II, Greathouse, D. V., Jude, A., Saberwal, G., Providence, L. L., & Andersen, O. S. (1994b) *J. Biol. Chem.* 269, 12567-12576.
- Lemmon, M. A., Flanagan, J. M., Treutlein, H. R., Zhang, J., & Engelman, D. (1992) *Biochemistry* 31, 12719-12725.
- Mattice, G. L. (1994) Ph.D. Thesis, University of Arkansas.
- Mattice, G. L., Koeppe, R. E., II, Providence, L. L., & Andersen, O. S. (1995) *Biochemistry* 34, 6827-6837.
- O'Brien, P. J., Jules, R. S., Reddy, T. S., Bazan, N. G., & Zatz, M. (1987) *J. Biol. Chem.* 262, 5210-5215.
- Ovchinnikov, Y. A., Abdulaev, N. G., & Bogachuk, A. S. (1988) *FEBS Lett.* 230, 1-5.
- Prosser, R. S., Davis, J. H., Dahlquist, F. W., & Lindorfer, M. A. (1991) *Biochemistry* 30, 4687-4696.
- Rance, M., Sørensen, O. W., Bodenhausen, G., Wagner, G., Ernst, R. R., & Wüthrich, K. (1983) *Biochem. Biophys. Res. Commun.* 117, 479-485.
- Randall, W. R. (1994) *J. Biol. Chem.* 269, 12367-12374.
- Schmidt, M. F. G. (1989) *Biochim. Biophys. Acta* 988, 411-426.
- Takeuchi, H., Nemoto, Y., & Harada, I. (1990) *Biochemistry* 29, 1572-1579.
- Tucker, W. A., Fletcher, T. G., & Hinton, J. F. (1993) *Biophys. J.* 64 (2, part 2), A299 (abstract).
- Urry, D. W. (1971) *Proc. Natl. Acad. Sci. U.S.A.* 68, 672-676.
- Vogt, T. C. B. (1994) Ph.D. Dissertation, University of Utrecht.
- Vogt, T. C. B., Killian, J. A., Demel, R. A., & De Kruijff, B. (1991) *Biochim. Biophys. Acta* 1069, 157-164.
- Vogt, T. C. B., Killian, J. A., De Kruijff, B., & Andersen, O. S. (1992) *Biochemistry* 31, 7320-7324.
- Williams, L. P., Narcessian, E. J., Andersen, O. S., Waller, G. R., Taylor, M. J., Lazenby, J. P., Hinton, J. F., & Koeppe, R. E., II (1992) *Biochemistry* 31, 7311-7319.
- Wüthrich, K. (1986) *NMR of Proteins and Nucleic Acids*, John Wiley and Sons, New York, NY.